Geophys. J. R. astr. Soc. (1982) 70, 415–433

Instabilities of fluid conduits in a flowing earth – are plates lubricated by the asthenosphere?

John A. Whitehead, Jr *Woods Hole Oceanographic Institution, Woods Hole, Massachusetts 02543, USA*

Received 1981 September 23; in original form 1981 May 30

Summary. A laboratory and theoretical study of the stability of conduits of buoyant fluid in a viscous shear flow has been conducted. The object of the study is to explain the formation of discrete islands in island chains such as the Hawaiian Emperor seamount chain, and to investigate a new method by which the variation of shear with depth in the mantle may be determined. The conduits were made by injecting oil into a more viscous oil of greater density. Initially a growing chamber of lower viscosity oil formed near the injector, but when the chamber got sufficiently large it rose as a buoyant spheroid. Behind this trailed a vertical cylindrical conduit through which fluid could continue to rise to the surface as long as the source continued. If the more viscous fluid was sheared laterally the conduit was gradually rotated to a more horizontal position. The diameter of the conduit increased with time due to a decreasing component of gravitational force along the axis of the conduit. When the conduit was tilted to more than 60° with the vertical, it began to go unstable by developing bumps which ultimately initiated a new chamber which rose to a new spot. In addition, if the Reynolds number of the conduit was greater than approximately ten, an axisymmetric wavy instability appeared in the walls of the conduit and the conduit had to be tilted less before a new chamber was initiated. If shear under the Pacific plate has to tilt buoyant mantle plumes to as much as 60° to form the relatively regular island chains associated with hot spots, most of the shear would be found in a zone with a vertical extent of less than 200 km.

1 Introduction

Wilson (1963) suggested that island chains such as Hawaii were formed as plates passed over a fixed region of the mantle where large amounts of magma were being produced. The essential concept is that the ultimate source is below most of the flow under the plates. Material then rises from this source because it has lower density than the material around it. It has been shown that the source regions for these hot spots move more slowly with respect to each other, for instance at rates of 0.8–2 cm yr^{-1} (Molner & Atwater 1973) than they do with respect to the plates. The ultimate source may be plumes of hot material rising from

the core–mantle boundary (Morgan 1971, 1972) or from the upper mantle–lower mantle interface (McKenzie & Weiss 1975) or elsewhere as reviewed by Dalrymple, Silver & Jackson (1973), but the concept that the source must be somehow disconnected from the rapidly moving plates near the surface of the Earth has persisted.

Finally, there is evidence, based upon various isotope measurements, that the material that forms mid-plate or 'hot spot' islands has long ago differentiated from material which upwells at spreading centres (O'Nions, Hamilton & Evensen 1980). This supports the notion that the 'plumes' feeding these islands are very localized since material that was once part of a plume is not found at spreading centres.

We wish to investigate a simple problem in fluid mechanics which we believe will shed light on the mechanism by which lower viscosity fluid buoyantly rises up through a shear zone. Clearly, if plumes in the mantle are 'hot' and viscosity decreases with increasing temperature, then plumes are low-viscosity regions, the only question is how low. Similarly, it is almost certain that the plumes are buoyantly rising up through denser fluid. Lastly, it is clear that if the hot spot sources have moved with respect to the plates, or vice versa, there must be a shear zone between the source and the plate. Thus the three features of buoyancy, lower viscosity and shear zone all seem to be essential elements in the dynamics of hot spots and their emergence at the surface of the Earth.

The effects of buoyancy and low viscosity are discussed by Whitehead & Luther (1975), who showed the way in which low-viscosity fluid buoyantly rises when injected through a small source into a high-viscosity host fluid of greater density which is at rest (both fluids being in the low Reynolds number parameter region). Initially the less viscous fluid pushes out into the host fluid, and its nose is subjected to a gradually increasing normal stress. The fluid first fills a spheroidal cavity at the site of injection and grows without rising very rapidly. Eventually the radius becomes large enough so that the spheroid rises buoyantly more rapidly than the rate of change of radius. The cavity appears to rise away from the source when this stage is reached, and as it does so, it trails behind a narrow feeder conduit as shown in Plate 1.

They further show that equations which describe the behaviour of a viscous fluid flowing in a cylindrical conduit with rigid walls together with a hydrostatic assumption can be combined to predict the radius r of a viscous vertical conduit in a much more viscous fluid. They found

$$r = \left(\frac{8\bar{\mu}Q}{\pi g\,\Delta\rho}\right)^{1/4} \tag{1.1}$$

where $\bar{\mu}$ is the viscosity of the fluid in the conduit, Q is the volumetric flux of the fluid, g is the force of gravity and $\Delta\rho$ is the density difference between the two fluids.

The effect of shear of the host fluid has only briefly been conjectured about. Where there is no shearing flow, the fluid rises vertically; however, it is reasonable to anticipate that a horizontal shear flow would cause the conduit to deviate from this vertical motion and assume an inclined position. As the inclination to the vertical increases, the buoyancy force causing the fluid to flow *along* the conduit decreases so that the velocity within the conduit decreases, and the radius increases to conserve mass. That is, if the conduit were inclined, the force of gravity would be replaced by its component in the direction of flow, hence

$$r = \left[\frac{8\bar{\mu}Q}{\pi g\,\Delta\rho\sin\theta}\right]^{1/4} \tag{1.2}$$

where θ is angle of the conduit with the horizontal (this definition of θ will be used throughout the paper).

Once the conduit is inclined to the vertical, there is a component of the buoyancy force perpendicular to the axis of the conduit, which causes the conduit itself to rise through the host fluid. Skilbeck & Whitehead (1978) used the formula of a rigid rod rising buoyantly through a viscous fluid to model this, i.e. the vertical velocity w is given by

$$w = (\ln a)\frac{g\,\Delta\rho\, r^2}{8\mu}(3 - \cos 2\theta) \tag{1.3}$$

where μ is viscosity of the host fluid and the parameter a is the aspect ratio of the rod (length to radius). When equations (1.2) and (1.3) are useful approximations, it seems inevitable that at sufficiently large angles to the vertical, it would be easier for the fluid to form a new cavity and rise vertically than to move up the small incline of the existing conduit. To see this, note that a small decrease in angle somewhere in the region of the smallest slope would lead to a greater radius (from 1.2) and hence the vertical velocity w (from 1.3) would be greater, causing an even smaller angle. The repetition of such a procedure might lead to the formation of island chains as was suggested by Skilbeck & Whitehead (1978). Using the above equations, they made some estimates of the angles and times necessary to be consistent with the spacing of the Hawaiian chain. It was found that this mechanism would be only consistent with relatively sharp slip zones (100 km or less) below the plates.

It is not known in detail how good a model these formulae are for real conduits of molten or partly melted material in the Earth. It probably has the appropriate dependence of viscosity of the host fluid (to the minus one power) and radius of the conduit squared. The dependence on the angle is more suspect. However, it is not the purpose here faithfully to model a complex natural intrusion, but rather to generate a plausible, and properly understood mechanical model using the simplest possible approach.

It is our purpose here to clarify and quantify the dynamics of tilted conduits for buoyantly flowing fluid using both theoretical considerations and laboratory experiments. However, before proceeding, brief mention will be made of a numerical calculation done by J. Skilbeck (private communication) which illustrates the reason why it was felt that shear would ultimately close off a pipe and initiate a new cavity. Caution is necessary because unrealistically simple equations were used and a class of instabilities which change the picture (see Section 2) were excluded. In this calculation the lateral advection of the pipe was due to a velocity profile of the form

$$u = u_0 \frac{\tan^{-1} z/L}{\tan^{-1} h/L}. \tag{1.4}$$

Such a velocity distribution is a solution for shear flow which satisfies $\partial/\partial z\,[\mu(\partial u/\partial z)] = 0$ if the viscosity field is parabolic, specifically of the form

$$\mu = \mu_0 \frac{(1 + z^2/L^2)}{(1 + h^2/L^2)}. \tag{1.5}$$

Thus the viscosity is at a minimum at $z = 0$. The letter h is the depth of the minimum viscosity (at $z = 0$) below the Earth's surface (where $\mu = \mu_0$), and L is the length scale of the viscosity variation. The relations (1.4) and (1.5) were the simplest continuous relations with a viscosity minimum that could be found. Although viscosity varies rather slowly in the formulation (you must go to $10L$ to get two orders of magnitude change in viscosity) the shear is extremely abrupt, 53 per cent of the deformation takes place between $z = \pm L$ (where the

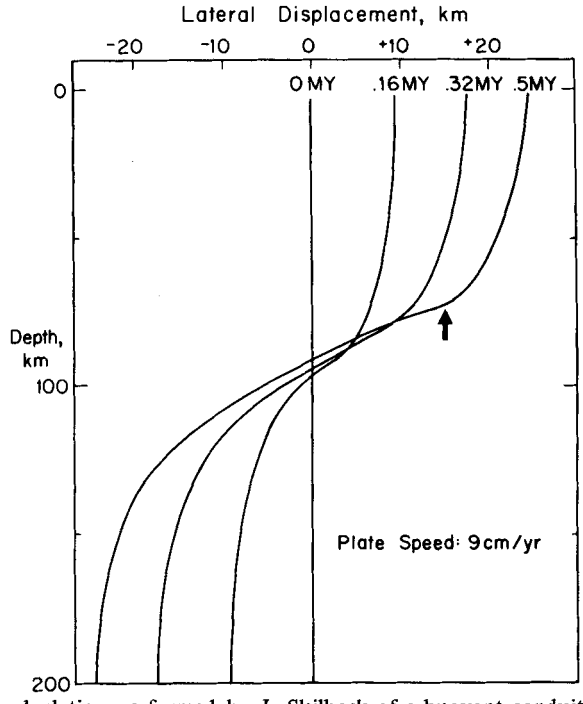

Figure 1. Numerical calculation performed by J. Skilbeck of a buoyant conduit that is being tilted by shear. At the point of the arrow the conduit reached zero slope shortly after 0.5 Myr.

viscosity has increased by a factor of 2), 75 per cent between $z = \pm 2L$ (where the viscosity has increased by a factor of 5), and 84 per cent between $z = \pm 3L$ (where the viscosity has increased by a factor of 10). All the above are for the case where $h = 10L$. *This fact alone makes it likely that if the asthenosphere has a significantly lower viscosity, a large amount of the shear under plates will occur there.*

The evolution of the figure of a conduit subject to the above viscosity and shear distribution, and subject to the radius given by (1.3) and vertical velocity of the pipe given by (1.4) is shown in Fig. 1, for $h = 100$ km, $L = 10$ km, $u_0 = 9$ cm yr^{-1}, $\mu_0 = 10^{21}$ poise (approximately 5×10^{18} cm s^{-1}), and $Q = 10^6$ cm^3 s^{-1}. The calculations were performed by specifying 100 Lagrangian points to describe the conduit and thereby integrating the above equation of motion in time steps of 10 000 yr starting with equation (1.4) to get a new lateral position, then going to (1.2), thence to equation (1.3) to determine new horizontal positions for the points. In equation (1.3) the local viscosity (equation 1.5) was used for each point. Fig. 1 shows the calculated evolution of this conduit for 160 000, 320 000 and 500 000 yr. Shortly thereafter, the two points nearest the arrow reached the same level and hence the radius (and vertical velocity) in this model became infinite. There was no reason to believe that invoking a more realistic set of equations, such as accounting for radius change in the continuity equation, would change this picture drastically. One can easily estimate that this would only be important for the last few calculations steps as angles get to be very small. Hence the conjecture of Skilbeck & Whitehead – that shear would tilt pipes and initiate a new cavity in finite time, was strongly supported.

2 Laboratory experiments

Skilbeck & Whitehead also described a number of preliminary experiments in which a feeder

conduit was generated in a closed container in the laboratory, and then tilted. It was reported that at an angle with the horizontal of less than approximately 35°, the conduit developed instabilities. Since these were not seen in the preceding numerical model, it was felt that further experiments were necessary to clarify the stability of conduits and their possible role in the formation of a new cavity. It was desired to subject the conduits to shear with a maximum at some clearly defined depth as this must be true under the plates. After a good deal of experimentation with pumps, sources, sinks and so forth, the apparatus shown in Fig. 2 was constructed and found to be satisfactory. It consists of a bottom deep annulus, with the radius of the inner wall of 16 cm, the outer wall 23 cm and a depth of 30 cm. Into this was suspended a second annulus upside-down – extending down into the lower annulus to 9 cm above the bottom, with a radius of the inner wall of 17 cm and a radius of the outer wall of 22 cm. The top annulus was connected to a bearing and motor so it was free to rotate at speeds of 0.20–1.0 mm s^{-1}. All walls were constructed of Plexiglas 0.1 cm thick which was simply curved and cemented. The base was $^3/_8$" methyl methacrylate with circular slots for the bottom annulus walls. At one point midway between the inner and outer wall a 0.5 cm diameter hole was drilled, and a 0.4 cm inner diameter, 0.5 cm outer diameter plastic tube was inserted to serve as a source of conduit fluid. This tube was connected to a precision positive displacement pump and a reservoir. The apparatus was filled with 10 $cm^2 s^{-1}$ silicon oil to a depth of 22 cm. The apparatus was therefore like a double annular Hele-Shaw cell. Oil near the top of the annulus moved with the top inner annulus. Oil near the bottom of the annulus remained almost stationary. There was a maximum shear zone near the bottom of the top annulus whose vertical extent was the width of the Hele-Shaw cell.

Before each experimental run was conducted the fluid in the annulus was thoroughly mixed to get rid of fossil conduits from the preceding runs. Since the fossil conduits contained small amounts of oil with viscosity less than 10 $cm^2 s^{-1}$, the mixing gradually decreases the viscosity of the oil in the annulus. Therefore, the viscosity of the fluid in the annulus was determined by timing the descent of a small plastic ball prior to each run. For the duration of the experimental programme the viscosity decreased less than 10 per cent.

The experimental procedure was to first leave the tank overnight after each run to allow the stirred fossil conduits to diffuse away. Then, next day the pump was turned on at the desired rate, a chamber formed, rose, and the conduit trailed behind. (Three viscosities were

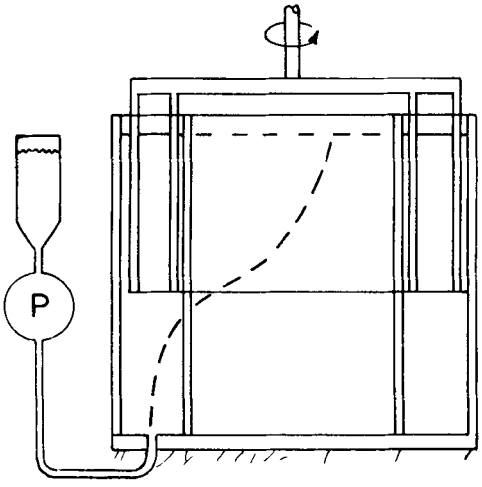

Figure 2. Experimental apparatus to produce a zone of maximum shear midway down through the fluid.

used for the conduit fluid, 0.01, 0.1 and 1 $cm^2 s^{-1}$, but the 1 $cm^2 s^{-1}$ conduits were so large that they never tilted enough to go unstable so results for the two lower viscosities are reported here.) Thereafter, fluid could rise through the conduit steadily. After that the upper annulus was rotated at a set rate. Photographs and movies were taken of the evolution of the conduit. The velocity of the annulus was then increased to the next level and the observations were repeated. Typically three to five rates of annulus rotation could be set in a day. After that, the pump was set to the next value of mass flux and the next experimental run was conducted during the following day, preceding which the tube which fed the lower viscosity oil was purged by air overnight, all top oil was skimmed off (with a bit of the oil below as well) after which the oil was thoroughly mixed. The following day's runs were conducted in the same manner.

Data were recorded by a 16 mm movie camera and a 35 mm camera. The conduits and chambers were viewed by shadowgraph. The light projected on to a screen 6 cm in front of the tank. Thin vertical (to within 1°) and horizontal level strips of adhesive tape were placed on the tank so the local direction of gravity could be determined on the movies and photographs. Seven pieces of adhesive tape 1 cm wide were also stuck as fiducial marks to the walls of the annulus to calibrate aberration due to the shape of the tank and the index of refraction of the oil and tank walls.

The marks were calibrated by inserting a 0.3175 cm metal rod into the annulus and measuring the vertical and horizontal size of the rod's shadow on the screen of the shadow-

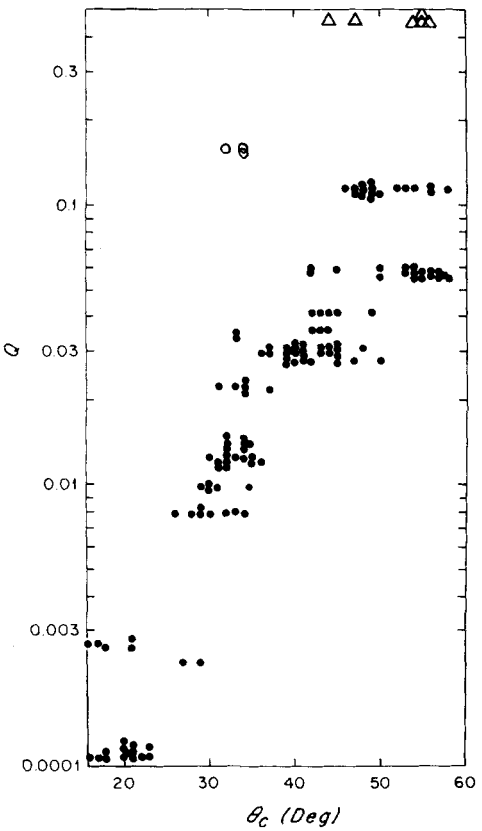

Figure 3. Critical angle versus mass flux for conduit fluid with a viscosity of 0.01 $cm^2 s^{-1}$. Annulus speeds are ○ – 1 mm; △ – 0.5 mm s^{-1}; ● – 0.25 mm s^{-1}.

graph. Many factors distorted the image on the screen slightly but the principal ones were bulging of the thin tank walls from hydrostatic pressure, and optical refraction from the many cylindrical surfaces of the tank. Corrections to the image on the screen of the shadowgraph were as much as a factor of 3 with an uncertainty of ± 25 per cent. Lengths reported here will be with that uncertainty.

The experiments provided answers to the following questions:

2.1 DO NEW CHAMBERS FORM AS SUGGESTED BY SKILBECK AND WHITEHEAD?

Yes, new chambers form if shear can tilt them sufficiently. The mechanism for the formation clearly resembled the instability mentioned in Skilbeck & Whitehead. Plate 2 shows photographs of typical instabilities and the subsequent initiation of new chambers.

Figs 3–5 show the parameter space covered in terms of mass flux and Reynolds number calculated in the conduit. Reynolds number was estimated using the formula $Q/\pi r\bar{\nu}$, where r is a radius of the vertical conduit (a discussion of the measurements of the radius will follow) and $\bar{\nu}$ is the kinematic viscosity of the fluid in the conduit. Most conduits were unstable but there were two different ways the conduits were stable. If the mass flux is very large, the conduits are so big and buoyant that the shear of the annulus never tilts them enough to achieve a critical angle. Such a case is shown in Plate 3(a). If mass flux is very small, the velocity in the conduit is so small that the conduit is perpetually passively stretched. Such a case is shown in Plate 3(b).

The angle of instability obviously varies in parameter space, but for numbers appropriate for the Earth, there is probably less variability since it is believed the Reynolds number span between 0.7 and 2.8 is most relevant as discussed below. In that case the critical angle was measured for 37 cases, and the angle was determined to be 32.2° with a standard deviation of only 2.32°.

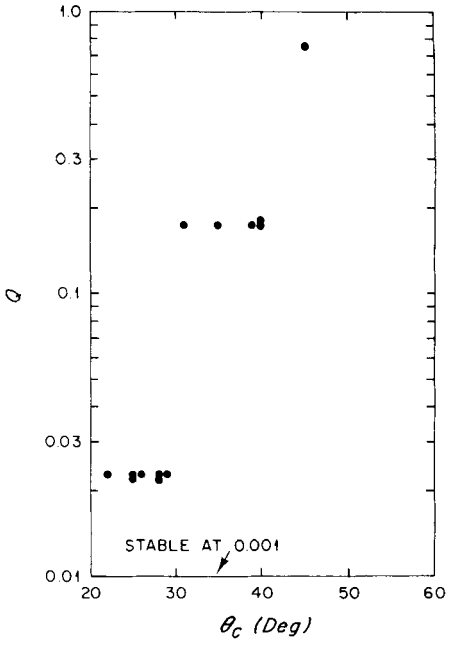

Figure 4. Critical angle versus mass flux for conduit fluid with a viscosity of 0.1 $cm^2 s^{-1}$.

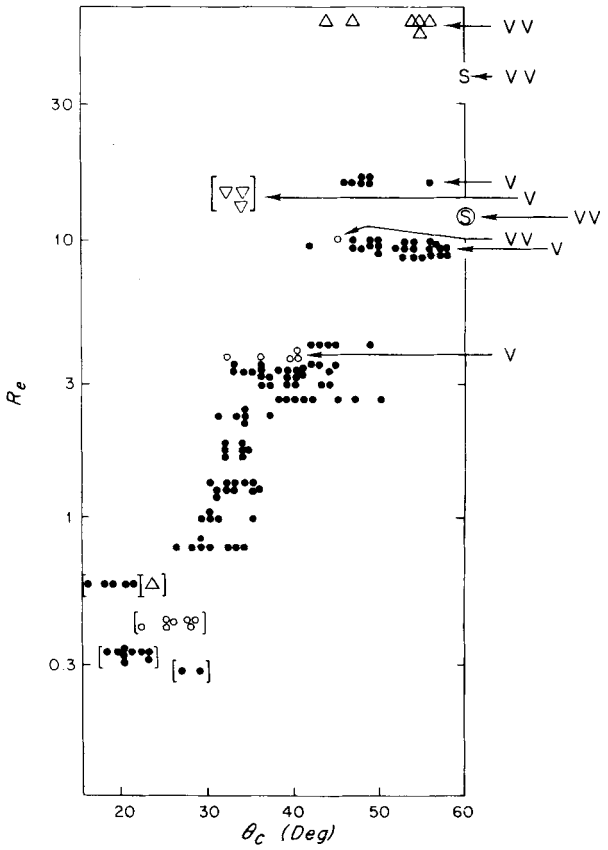

Figure 5. Critical angle versus Reynolds number for all experiments. V denotes a varicose conduit, VV denotes a very varicose conduit. Viscosities (in centistoke, $s = 0.1\ \mathrm{cm^2\,s^{-1}}$) and annulus velocities (in $\mathrm{mm\,s^{-1}}$) are: ● – $\bar{\mu} = 1.0, v = 0.25$; △ – $\bar{\mu} = 1.0, v = 0.50$, ▽ – $\bar{\mu} = 1.0, v = 1.0$; ○ – $\bar{\mu} = 10.0, v = 0.25$; Ⓢ – $\bar{\mu} = 1.0, v = 0.25$ (no instability observed). In both of the last two cases the conduit never tilted more than the angle shown. The data in brackets are estimated to have velocities in the conduits smaller than the annulus velocities and therefore the conduit was somewhat dominated by stretching.

There are two reasons why this is most appropriate for the Earth: when the flow rate (and hence Reynolds number) was less, the conduits were so small that they were advected by the shear more rapidly than they could buoyantly move through the shear so that the conduit is perpetually passively stretched. Although sometimes this completely stabilized the conduit, there were cases where the conduit was unstable but where the angle of instability was small because the stretching seemed to tend to stabilize the conduit. A criterion is derived in Section 4 for when this might occur, and experimental runs where this criterion was met are shown in brackets. It is also shown in Section 4 that this is unlikely to occur in the Earth for the larger hot spots.

Second, when the Reynolds number is larger than 2.8, a varicose instability (see Section 2.3) was obvious. The photographs in Plate 2 are actually very close to this limit. This instability clearly changes the critical angle as discussed in Section 2.3 and is shown to be unlikely for the Earth in Section 4.

2.2 WHAT IS THE SPACING OF THE CAVITIES?

The distances between all cavities are shown for all runs in Fig. 6. Even though there are

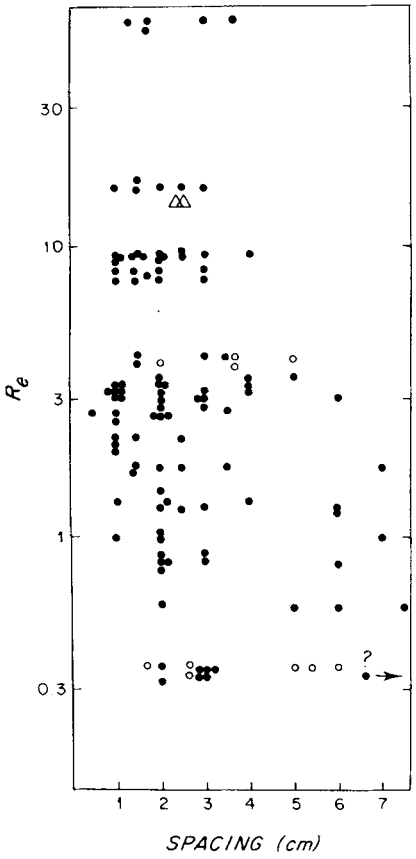

Figure 6. Spacing of the cavities as a function of Reynolds number.

vastly different viscosities and pumping rates the spacing is always of the order of the length scale of the shear even though there is considerable scatter. We were surprised that the angle has less scatter than spacing. This is due to scatter in spacing which is produced by interactions between adjacent cavities. For instance, there was a clear bimodal nature of the clustering at low Reynolds number which is produced because two instabilities occur almost simultaneously and then sweep the conduit vertically. The stochastic nature of the spacing is further heightened by the fact that the cavities have a much larger length scale than the small bumps on the conduit. This results in many bumps competing to become the next large chamber with only one bump (or occasionally two and, in one case, three) the winner. It would be interesting to see if there is some parameter space where conduits are the same size as chambers and to see if this leads to regular spacing.

2.3 DOES THE VARICOSE INSTABILITY CHANGE THE CRITICAL ANGLE AND SPACING OF THE CAVITIES?

The answer is yes, but first it is necessary to discuss the varicose instability. It appears to be an instructive transition of a laminar flow to a more turbulent flow. As the Reynolds number gets larger, the flow gets more strongly governed by Bernoulli's law. This gives an obvious source to the instability because if the conduit becomes slightly pinched somewhere, the velocities will have to increase at the pinch, and pressure will be lowered by Bernoulli's law.

This will tend to draw the viscous outer fluid inward and increase the pinch. This instability changes the angle of chamber formation significantly as Fig. 6 shows through the obvious mechanism of producing a local region with a small angle. Because of this, it is harder to measure the angle of instability for varicose conduits since they are continually deformed.

2.4 DOES THE RADIUS OF THE CONDUIT AGREE WITH THE PREDICTION (EQUATION 1.1)?

The conduits mysteriously produced a shadow which was approximately four to six times larger than the predicted size of the conduits from equation (1.1). This was puzzling because the equation and the derivation was so straightforward that it was unlikely to be wrong. The following experiment resolved the mystery. Plate 4(a) shows a photograph of a conduit of clear oil in front of lined paper at a 45° angle. The size of the conduit is apparent from the width of the refracted lines. A shadowgraph of the conduit lies nearby. Shortly thereafter dyed oil was fed to the source. The dyed region would subsequently mark the width of the region of sensible flow. Plate 4(b,c) shows the dyed fluid 1 and 2 min after introduction (vertical velocity in the conduit was 1.5 cm s at the centre, so after 1 min the region of the conduit which had most of the flow would be filled). By 1 min, and certainly by 2 min, the dyed fluid should have essentially filled the conduit, yet the dyed conduit is much smaller (less than half) than the region of refraction of the 45° lines and smaller still than the shadowgraph thickness.

In addition, the width of the dyed region agreed more closely with 1.1 than did the shadowgraph, although it was still somewhat larger (possibly due to some inward diffusion of viscous fluid). Therefore, for the purposes of estimating a radius r for the Reynolds number, we adopted a radius r one-third of the measured shadowgraph radius for the 0.01 $cm^2 s^{-1}$ experiments and 1.3 the measured radius for the 0.1 $cm^2 s^{-1}$ experiments (since the conduit radius was much larger). Although this is a relatively crude correction, the consequences are not grave since the Reynolds number varied over two orders of magnitude.

Possibly the low viscosity fluid diffuses radially at rather high rates (based upon what we could consider a 'reasonable' diffusivity of 10^{-4} $cm^2 s^{-1}$) to make the refractive edge of the conduits. Plate 4(d), photographed after 10 min, hints that there is significant lateral diffusion by the fuzziness of the edge of the pipe. Possibly the large concentration gradients make a non-linear and large diffusivity, this we could not verify, but the evidence for large diffusion seems strong.

3 Stability of a tilted conduit

The experiments suggest that a conduit is unstable to very small perturbations at some finite angle. Thus, a stability analysis is appropriate. This analysis, although it is relatively comprehensible, unfortunately relies on two assumptions which are severe enough to cast doubt that the results can be usefully compared with the stability properties of a tilted conduit in the Earth in detail. However, it does lead to an angle of instability which is within 20 per cent of that observed experimentally. In addition, the model illustrates some of the force balances that would probably be operating in any tilted conduit of low viscosity fluid and, since it is wise to study the simplest models first, we feel this analysis is the best first step.

Consider an almost straight conduit which initially is tilted at some angle θ_0 and located at $h(x, t) = z$ so (1.3) is rewritten as

$$\frac{\partial h}{\partial t} = \frac{g\Delta\rho}{8\mu} \ln a r^2 (3 - \cos 2\theta) \tag{3.1}$$

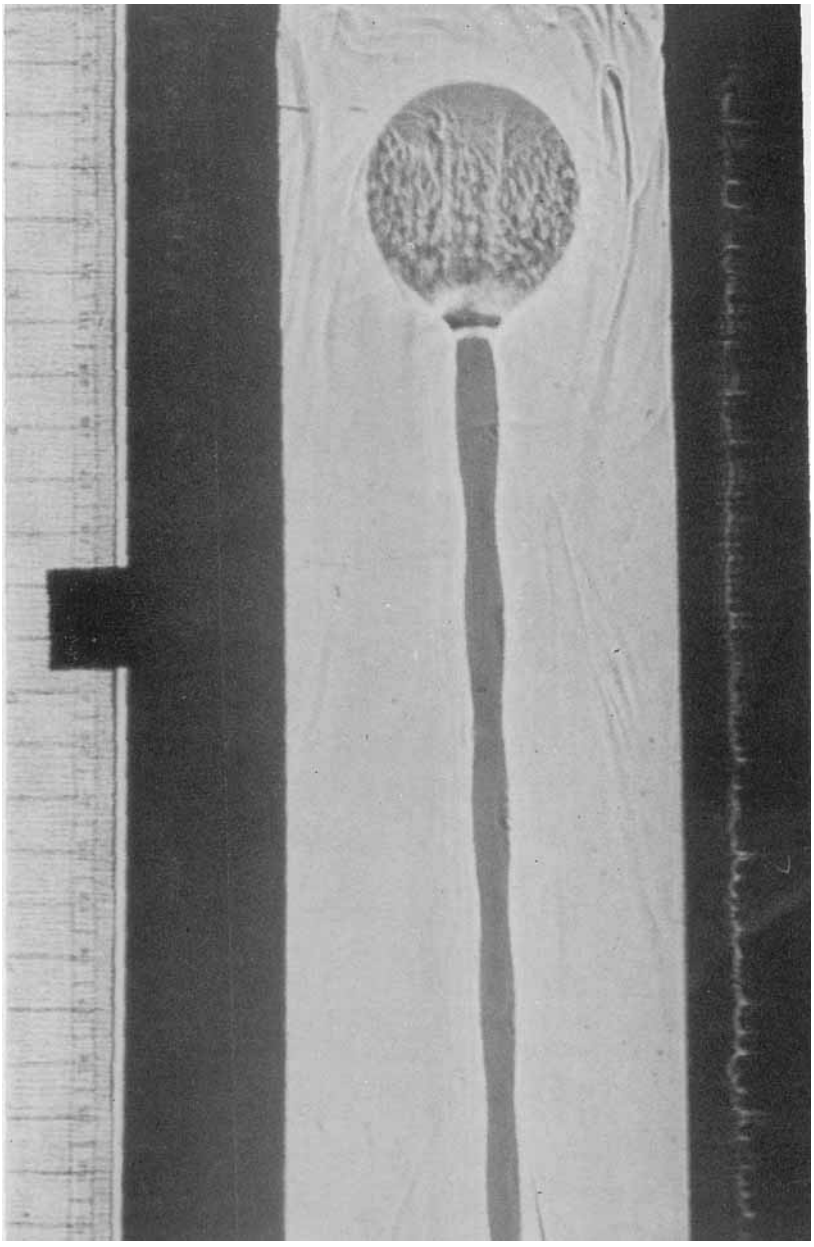

Plate 1. The cavity and conduit formed as viscous fluid rises buoyantly from a localized source through a much more viscous fluid.

[*facing page* 424]

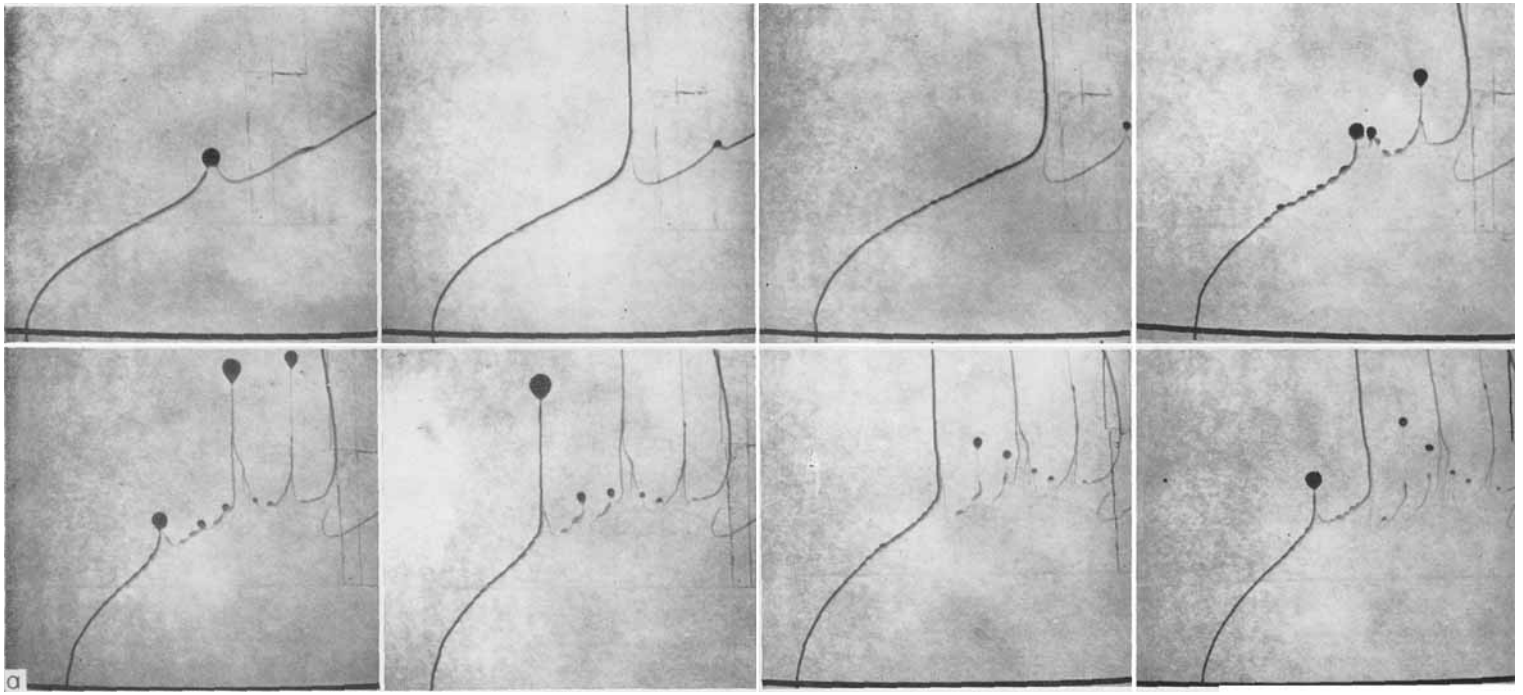

Plate 2. Instabilities of tilted conduits: (a) evolution of a typical laminar conduit (1 min between photos proceeding left to right), Reynolds number is 2.5; (b) shadowgraph of a varicose conduit being tilted and the formation of a new chamber 3 min later, Reynolds number is 9.8.

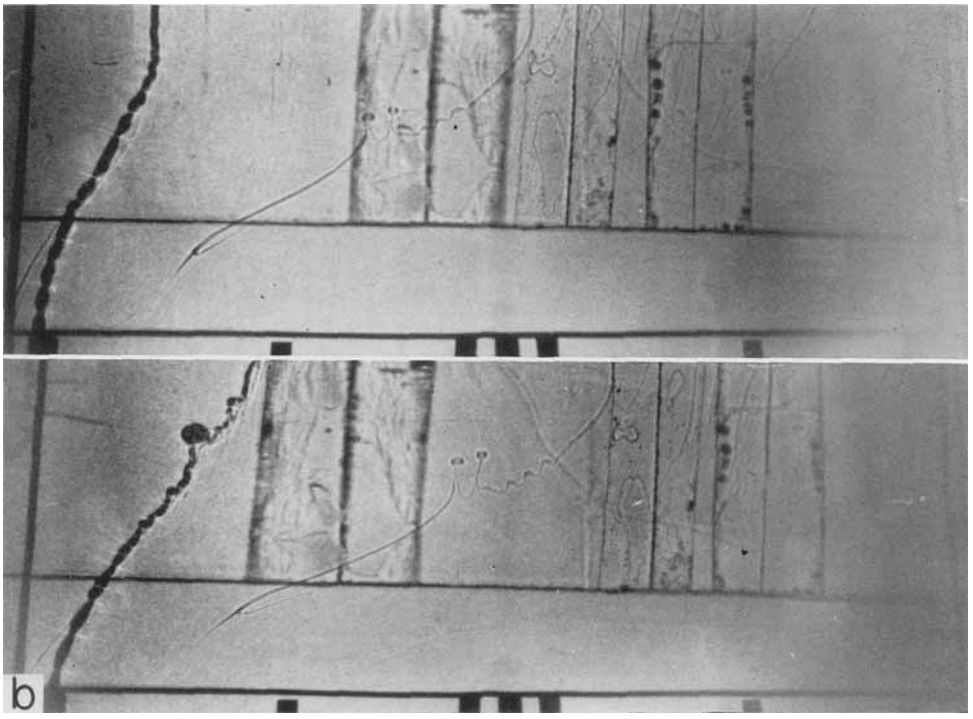

Plate 2. (b)

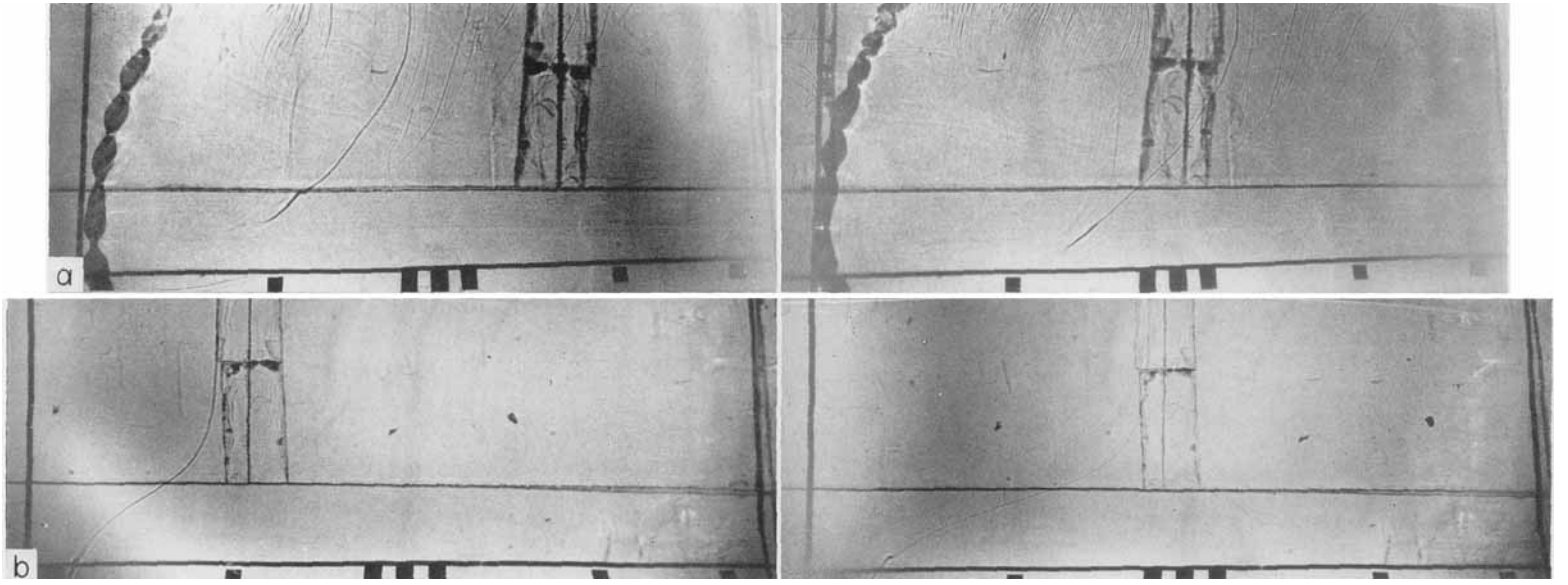

Plate 3. Two conduits that were not unstable: (a) mass flux very large (photos taken 5 min apart); (b) mass flux very small.

Plate 4. Optical size of the conduit: (a) and dyed size of the conduit after 1 min (b), 2 min (c) and 10 min (d).

where slope is defined as

$$\tan\theta = \frac{\partial h}{\partial x}. \tag{3.2}$$

The parameter $\ln a$ is the aspect ratio of the radius. Since this parameter varies weakly with a, this will be henceforth regarded as a constant of about 5 for purposes of simplification.

Continuity of fluid in the conduit is

$$\frac{\pi \partial r^2}{\partial t} = -\cos\theta \frac{\partial Q}{\partial x}. \tag{3.3}$$

Volumetric flux of the fluid through the conduit is to be given by the formula for flow through a pipe, i.e.

$$Q = \frac{\pi r^4}{8\bar{\mu}} \frac{\partial p}{\partial \gamma}$$

where

$$\frac{\partial p}{\partial \gamma}$$

is the pressure gradient at the centre of the fluid along the conduit and $\gamma = x/\cos\theta$.

As before, $\bar{\mu}$ is the viscosity of the conduit fluid and μ is the viscosity outside. For our conduits $\partial p/\partial\gamma$ is equal to the buoyancy force $g\Delta\rho \sin\theta$ plus any pressure due to the fact that the conduit is shrinking, swelling or twisting. We have found it necessary to retain the pressure resistance exerted by the viscous fluid outside the conduit as the radius expands or shrinks for reasons which will become apparent at the end of the analysis. For the moment this will be represented by $E\partial r/\partial t$. The constant E is determined in the Appendix and discussed after equations (3.14) and (3.15).

The formula for volumetric flux is thus:

$$Q = \frac{\pi r^4}{8\bar{\mu}} g\Delta\rho \sin\theta + E\frac{\partial r}{\partial t}$$

and (3.3) reads

$$\frac{\pi \partial r^2}{\partial t} = -\cos\theta \frac{\pi}{8\mu}\left[g\Delta\rho \frac{\partial}{\partial x} r^4 \sin\theta + \frac{\partial}{\partial x} r^4 E \frac{\partial r}{\partial t}\right]. \tag{3.4}$$

Expanding in a power series of ϵ,

$$h = h_0 + \epsilon\tilde{h} + 0(\epsilon^2)$$

$$r = r_0 + \epsilon\tilde{r} + 0(\epsilon^2)$$

$$\theta = \theta_0 + \epsilon\tilde{\theta} + 0(\epsilon^2).$$

For $\epsilon \ll 1$ the zeroth-order solution is a straight conduit rising at a constant rate

$$h_0 = \tan\theta_0 x + \ln a \frac{g\Delta\rho}{8\mu} r_0^2 (3 - \cos 2\theta_0) t \tag{3.5}$$

$$r_0 = \left(\frac{8\bar{\mu}Q}{\pi g \Delta\rho \sin\theta_0}\right)^{1/4}. \tag{3.6}$$

Hence, θ_0 and r_0 do not change with time.

The $0(\epsilon^1)$ terms are the linear stability equations,

$$\frac{\partial \tilde{h}}{\partial t} = \frac{g\Delta\rho}{4\mu} \ln a \, (r_0^2 \sin 2\theta_0 \, \tilde{\theta} + r_0(3 - \cos 2\theta_0)\tilde{r}\,, \tag{3.7}$$

$$\sec^2\theta_0 \tilde{\theta} = \frac{\partial \tilde{h}}{\partial x}\,, \tag{3.8}$$

$$2\pi r_0 \frac{\partial \tilde{r}}{\partial t} = -\left[\frac{\pi g \Delta\rho}{8\bar{\mu}}\left(r_0^4 \cos^2\theta_0 \frac{\partial \tilde{\theta}}{\partial x} + 4r_0^3 \sin\theta_0 \frac{\partial \tilde{r}}{\partial x}\right)\right] - \frac{\pi r_0^4}{8\bar{\mu}} \cos\theta_0 E \frac{\partial^2 \tilde{r}}{\partial x \, \partial t}\,. \tag{3.9}$$

We will represent $\tilde{h} = \exp[i(\sigma t + kx)]$. Then (3.8) requires that

$$\tilde{\theta} = \cos^2\theta_0 ik \exp[i(\sigma t + kx)]$$

and $\tilde{r}$ can be written as

$$\tilde{r} = r' \exp[i(\sigma t + kx)]\,.$$

Substitution and a small amount of manipulation allows one to see that r' obeys the following equations

$$i\sigma = iAk + Br' \tag{3.10}$$

$$i\sigma r' = Ck^2 - ikDr' \tag{3.11}$$

where

$$A = \ln a \frac{g\Delta\rho}{4\mu} r_0^2 \sin 2\theta_0 \cos^2\theta_0 \qquad (= \partial w/\partial\tilde{\theta}) \tag{3.12}$$

$$B = \ln a \frac{g\Delta\rho}{4\mu} r_0 (3 - \cos 2\theta_0) \qquad (= \partial w/\partial\tilde{r}) \tag{3.13}$$

$$C = \frac{g\Delta\rho}{16\bar{\mu}} r_0^3 \cos^4\theta_0 \left(1 + \frac{r_0^3 k^3 \mu \cos^3\theta_0}{16\bar{\mu}}\right)^{-1} \qquad (= \partial Q/\partial\tilde{\theta}) \tag{3.14}$$

and

$$D = \frac{g\Delta\rho}{4\bar{\mu}} r_0^2 \sin\theta_0 \cos\theta_0 \left(1 + \frac{r_0^3 k^3 \mu \cos^3\theta_0}{16\bar{\mu}}\right)^{-1} \qquad (= \partial Q/\partial\tilde{r})\,. \tag{3.15}$$

We show in the Appendix how the constant E results in the term $r_0^3 k^3 \mu \cos^2\theta_0/16\bar{\mu}$ in equations (3.14) and (3.15). This is pressure resistance due to the outer viscous fluid due to a change in radius. Note that it is negligible for small k. The coefficients A–D have the following physical meanings: A is the change in the vertical velocity of a conduit due to change in angle. B is the change in the vertical velocity of a conduit due to change in radius. C is the change in the mass flux (which then changes the radius due to continuity) due to change in slope and radius (because of the denominator term) and D is the change in the mass flux due to the spatial variation in radius.

In (3.10) and (3.11) the two unknowns are r' and σ. The former can be eliminated from (3.10) and (3.11) to find the equation which governs σ:

$$(\sigma - Ak)(\sigma + Dk) = -BCK^2 \tag{3.16}$$

which has roots

$$\frac{\sigma}{k} = \frac{(A-D)}{2} \pm \left(\frac{(A+D)^2}{4} - 4BC\right)^{1/2}. \tag{3.17}$$

Our objective is to find when imaginary (growing or decaying) values of σ are possible. Since A, B, C and D are real and positive, the only time we get imaginary roots is when

$$(A+D)^2 < 4BC. \tag{3.18}$$

To determine when this happens, note that only C and D have values of k in the denominator. We first look at the limit of small k, more specifically

$$k \ll \left(\frac{16\bar{\mu}}{\mu}\right)\frac{1}{r_0 \cos\theta_0}.$$

This limit is the long wavelength limit and does not have its pressure drag very accurately modelled by the analysis of the Appendix. Since it produces no pressure drag in this limit, the critical angle is probably underestimated. At this point, it is useful to assume $\bar{\mu} \ll \mu$. Since (3.12–3.15) are real, the criterion of a growing disturbance is

$$\frac{\sin^2\theta_0}{\cos^2\theta_0(3 - \cos 2\theta_0)} < \frac{\bar{\mu}}{\mu}(\ln a).$$

For small θ_0, this reduces to

$$\theta_0 < 2\left(\frac{\bar{\mu}}{\mu}\right)^{1/2}(\ln a)^{1/2}.$$

Thus the critical angle is extremely small for small wavenumbers. Will a larger wavenumber require a larger angle? The answer is yes, and now the pressure resistance term begins to become important. In the range

$$\left[\left(\frac{16\bar{\mu}}{\mu}\right)^{1/3}\frac{1}{\cos\theta_0 r_0}\right] < k < r_0^{-1}$$

the terms in the denominator of C and D are greater than one, but $r_0 k$ is still small, hence D is still much greater than A, and the criterion for a growing disturbance is

$$\sin^2\theta_0 < \frac{r_0^3 k^3}{16}\ln a(3 - \cos 2\theta_0)\cos^5\theta_0.$$

For $\theta_0 \ll 1$ this reduces to

$$\theta_0 < \frac{(2r_0 k)^{3/2}}{4}\sqrt{\ln a}.$$

Using (3.6)

$$\theta_0 < (2k)^{12/11}\left(\frac{8\bar{\mu}Q}{\pi g \Delta\rho}\right)^{3/11}\frac{(\ln a)^{8/11}}{4}.$$

Thus as k increases, so does θ_0 for instability. Finally, when k becomes on the order of r_0^{-1}, $r_0 k$ will be one, in which case the term A (3.12) is the same size as D (3.15) and the criterion for a growing disturbance is

$$\left(\ln a \frac{\sin 2\theta_0 \cos^2 \theta_0}{4} + 4 \sin \theta_0\right)^2 < \ln a (3 - \cos 2\theta_0) \cos^5 \theta_0 .$$

If $\ln a$ is 5 ($a \cong 150$) the angle is approximately 35°. This is the largest angle which the theory predicts to be unstable. The pressure resistance is reasonably well modelled in this limit in the Appendix, and since the theory gets numbers that are approximately in the right range, hopefully the theoretical model is correct.

The mechanism for the instability is clear as sketched in Fig. 7. The terms BC must be greater than $(A + D)^2$. B is the change in upward velocity due to a change in radius and C is the change in radius due to change in angle. These were the two factors discussed in Skilbeck & Whitehead and in the computer experiments which led us to expect a zero slope in finite time. The terms A and D lead only to a travelling wave, i.e. oscillatory solution (σ real), which is very vigorous for small k, but develops pressure resistance for larger k so that the B and C terms can become important. The pressure resistance is felt most acutely by the D term (change in mass flux due to change in radius) and also (but less so) by the C term (change in mass flux due to change in angle and radius).

4 Application to the Earth

Let us assume that the viscosity of the parent material under a hot spot is unknown and that various volumetric fluxes correspond to different hot spots. We first ask when will the rate of vertical rise be faster than the lateral advection at an angle of 30° so that a pipe would not get tilted over that far, i.e. $w > u(\partial\eta/\partial x)$. If this happens we do not expect the tilt instability to develop unless there is a varicose instability.

Using equation (1.3) for w, (1.2) for r_0, we find

$$\ln a \left(\frac{g \Delta\rho \bar{\mu} Q}{8\pi \sin\theta}\right)^{1/2} \frac{3 - \cos 2\theta}{\mu} > u \tan\theta .$$

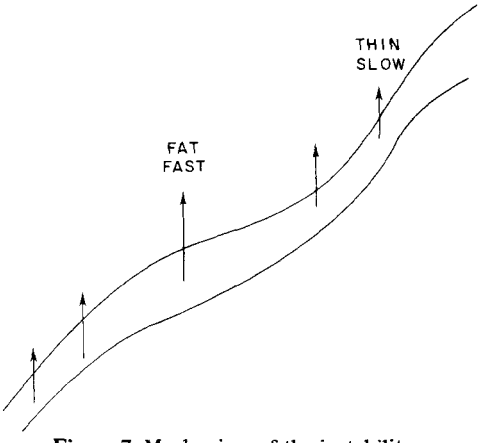

Figure 7. Mechanism of the instability.

For $\theta = 30°$, $g\Delta\rho \equiv 10\,\mathrm{g\,s^{-2}\,cm^2}$, $\ln a = 3$, $u = 10^{-7}\,\mathrm{cm\,s^{-1}}$ and $\bar{\mu} = 10^{18}$ poise, $\mu Q > 5.8 \times 10^{29}$. Expected values of μ would be less than 10^{22} poise since the glacial rebound data imply a mantle viscosity of that value (Cathles 1975; Peltier 1976). Expected value of Q would be $10^6\,\mathrm{cm^3\,s^{-1}}$ or less since this is the approximate value of Q for the Hawaiian chain, which is the biggest hot spot. The inequality is not satisfied for these values or any lower values hence it is likely that any mantle plume will not be able to maintain itself erect in the presence of mantle shear and will be tilted down to 30° so the instability studied here will develop.

Next we will calculate whether the varicose instability is to be expected. To answer this we will say that maximum vertical velocity in the pipe is

$$w = g\Delta\rho\, r_0^2/4\bar{\mu}$$

(see Whitehead & Luther 1975 – the equation between 16 and 17). Using (1.2) and $\theta = 90°$ the Reynolds number is

$$\mathrm{Re} = \frac{wr_0}{\bar{\mu}} = \frac{g\Delta\rho r_0^3}{4\bar{\mu}^2} = \frac{1}{4}\left[g\Delta\rho\left(\frac{8Q}{\pi}\right)^3 \mu^{-5}\right]^{1/4}$$

from (3.6). Setting $\mathrm{Re} = 10$ and $g\Delta\rho = 10\,\mathrm{g\,s^{-2}\,cm^2}$

$$\left(\frac{Q^3}{\bar{\mu}^5}\right) > (40)^4 \times \frac{1}{10}\left(\frac{\pi}{8}\right)^3 = 1.6 \times 10^4$$

or more for instability.

Using $Q = 10^6$, the pipe viscosity must be less than 5.74 poise which is lower than most surface lavas (Murase & McBirney 1973).

Thus it seems unlikely that either of the above possibilities could eliminate or alter the tilting of pipes that feed hot spots. Unless the convection is very much like roll convection (Richter & Parsons 1975) the instability of plumes is likely.

The most essential element for the considerations which we have discussed here is that rising fluid under a hot spot has lower viscosity than mantle material at the level of the greatest shear. The notion of a small lubricated conduit is compatible with the isotope evidence reviewed, for instance, by O'Nions *et al.* (1980) that the hot spot material has been differentiated from material that feeds spreading centres for a very long time.

One problem with the notion of a deep source of lower viscosity material is the commonly accepted idea that the mantle is probably composed of material whose melting curve as a function of temperature and pressure is considerably hotter than the estimate of temperature of the mantle. According to this notion if there is any melted material it would be found in the upper mantle, most likely at 100 km with much less melted, or partially melted material further down (Stacey 1975). One way melt could be formed at depths greater than 100 km is through a chemically differentiated mantle (Anderson 1977) which has been advocated by Schubert & Young (1976) (see also Schubert 1979) to prevent the core from freezing and to retain as valid the glacial rebound estimates of mantle viscosity of 10^{24} poise (Cathles 1975; Peltier 1976). Possibly conduits similar to those discussed here leach material from one of the layers, maybe even from the core.

The Hawaiian Emperor seamount chain is undoubtedly the hot spot which has been most regularly operating for the longest time. Crough (1978) has shown strong evidence that the islands associated with a number of hot spots are only small-scale manifestations of a larger structure which produces swells around the spots. The bathymetric and gravity data are consistent with the lithosphere being heated and therefore thinned to a depth equivalent to

approximately 25 M yr old crust. The swells are typically 1000 km broad and have been cited as evidence of a wide plume from substantial depth in the mantle. This interpretation is weakened by the fact that the swell only extends a short distance in front of the hot spot. It is further weakened by the lack of sideways scatter of the island chain which implies a very symmetrical plume. Certainly convection at large Rayleigh numbers is not so symmetric (Whitehead & Parsons 1976).

An alternate interpretation is that after chambers have formed near the shear maximum they rise only a small distance before the relatively larger vertical viscous resistance they encounter causes them to extensively flatten out. This aspect was not modelled in our experiments. Some chamber fluid then spreads out laterally and heats the base of the lithosphere rather quickly while the melt near the centre rises through the lithosphere by solid processes, i.e. crack propagation, stoping, etc. This interpretation is, however, weakened by evidence that there is no sign of fossil hot spot materials at spreading centres (O'Nions *et al.* 1980).

The notion that the islands are evenly spaced is clearly over-simplified. Fig. 8(b) shows the depth along the track shown in Fig. 8(a) which is the track of shallowest depth from Hawaii to the Aleutian Trench. One immediately sees that the island chain is clearly not a ridge although there are four ridge-like clusters at: (1) Hawaiian Islands, (2) French Frigate Shoals, (3) near the turn at Koko Seamount and (4) near Suike Seamount. The length scale of this ridge clustering is 500 km. There are a number of other length scales. The predominant one is approximately 100 km which is the size of a typical island or seamount. Then there is a third length scale of approximately 30 km which is the size of an individual volcano. Fig. 9

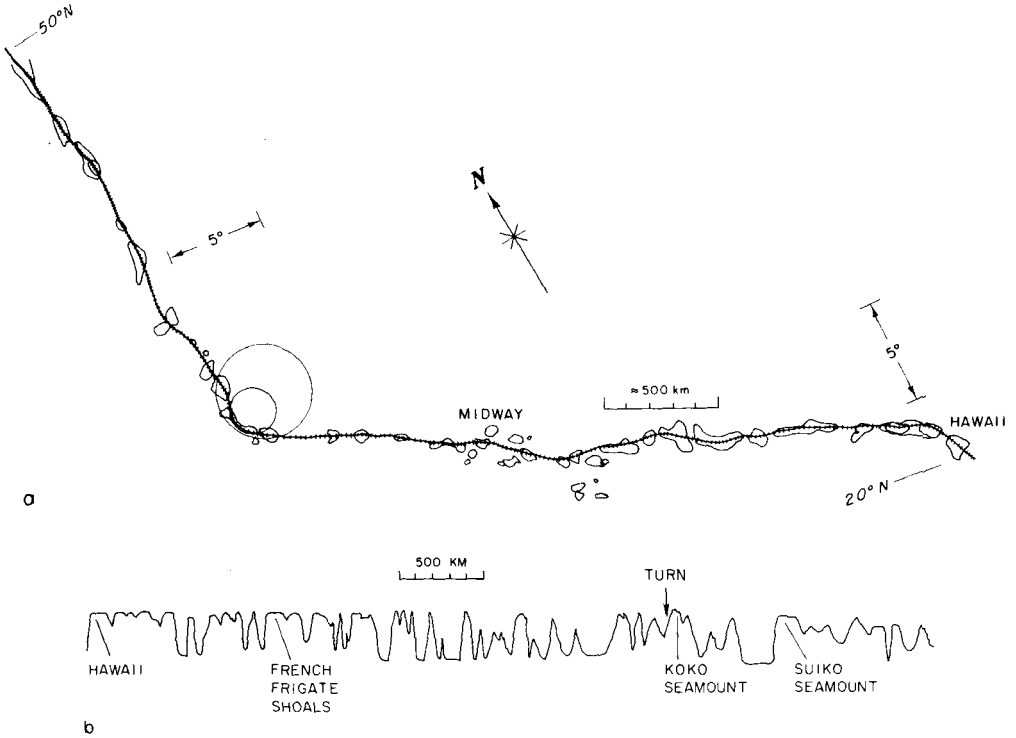

Figure 8. (a) The shallowest track along the Hawaiian Emperor seamount chain. The 1000 m contours are shown. (b) Bathymetry along the shallowest track.

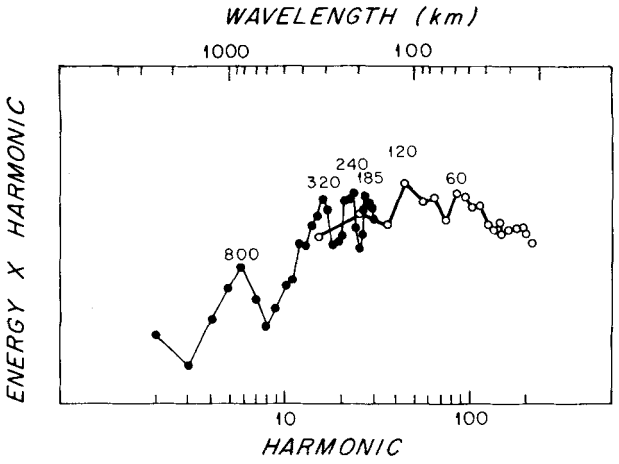

Figure 9. Spectrum of the bathymetry along the shallowest track of the Hawaiian Emperor seamount chain.

shows the spectrum of the bathymetry in Fig. 8(b). It has been smoothed by a ten-point mean for harmonics 10–200 and by a three-point running mean for harmonics 2–30. There is a broad bulge over a k^{-1} slope between wavelengths 45–200 km above which the spectrum begins to level off although there are local peaks at 60, 120, 185, 240, 320 and 800 km wavelengths, respectively. Resolution of the individual volcanoes is beyond the power of this method, but at approximately 30 km a peak would be expected.

We note that if the low viscosity lavas form above the shear zone due to fractionation processes a mechanism of Rayleigh–Taylor instability, as discussed by Marsh (1979), for island arcs may be more relevant to the lavas themselves. In that mechanism the spacing of the magma source is related to the viscosity ratios of the two fluids and the volume of the original magma chamber. Nonetheless the fluid at the shear maximum below the chamber will still be tilted and probably undergo some process like the one described here. Possibly the Marsh mechanism generates the close spacing between individual volcanoes (30 km on average), i.e. there is a Rayleigh–Taylor instability on the tops of 'plume' chambers. Meanwhile, the spacing between islands, which are aggregates of volcanoes, is determined by the processes described here. In such a case the length of the shear zone under plates is still likely to be 100 km or less to be compatible with spacings.

As Skilbeck & Whitehead mentioned, the notion of a shallow slip zone under the plates is not new. A variety of considerations dealing with force balances have recently reinforced this notion (Richter & McKenzie 1978). This is also reinforced by the sharpness of the bend in the Pacific hot spots. For instance, the radius of curvature of the bend in the Hawaiian Emperor seamount chain is somewhere between 100 and 200 km. Unless the hot spot fluid can melt its way directly through the shear zone, it is difficult to reconcile this sharp curvature (see Fig. 8a) with a shear zone over 200 km deep.

Acknowledgments

Support was given to this project from the Geophysics Division, National Science Foundation under grant EAR78-12927. Sincere thanks are extended to Robert Frazel for his valuable work on the experiment. This manuscript is Woods Hole Oceanographic Institution Contribution No. 4882.

approximately 25 M yr old crust. The swells are typically 1000 km broad and have been cited as evidence of a wide plume from substantial depth in the mantle. This interpretation is weakened by the fact that the swell only extends a short distance in front of the hot spot. It is further weakened by the lack of sideways scatter of the island chain which implies a very symmetrical plume. Certainly convection at large Rayleigh numbers is not so symmetric (Whitehead & Parsons 1976).

An alternate interpretation is that after chambers have formed near the shear maximum they rise only a small distance before the relatively larger vertical viscous resistance they encounter causes them to extensively flatten out. This aspect was not modelled in our experiments. Some chamber fluid then spreads out laterally and heats the base of the lithosphere rather quickly while the melt near the centre rises through the lithosphere by solid processes, i.e. crack propagation, stoping, etc. This interpretation is, however, weakened by evidence that there is no sign of fossil hot spot materials at spreading centres (O'Nions *et al.* 1980).

The notion that the islands are evenly spaced is clearly over-simplified. Fig. 8(b) shows the depth along the track shown in Fig. 8(a) which is the track of shallowest depth from Hawaii to the Aleutian Trench. One immediately sees that the island chain is clearly not a ridge although there are four ridge-like clusters at: (1) Hawaiian Islands, (2) French Frigate Shoals, (3) near the turn at Koko Seamount and (4) near Suike Seamount. The length scale of this ridge clustering is 500 km. There are a number of other length scales. The predominant one is approximately 100 km which is the size of a typical island or seamount. Then there is a third length scale of approximately 30 km which is the size of an individual volcano. Fig. 9

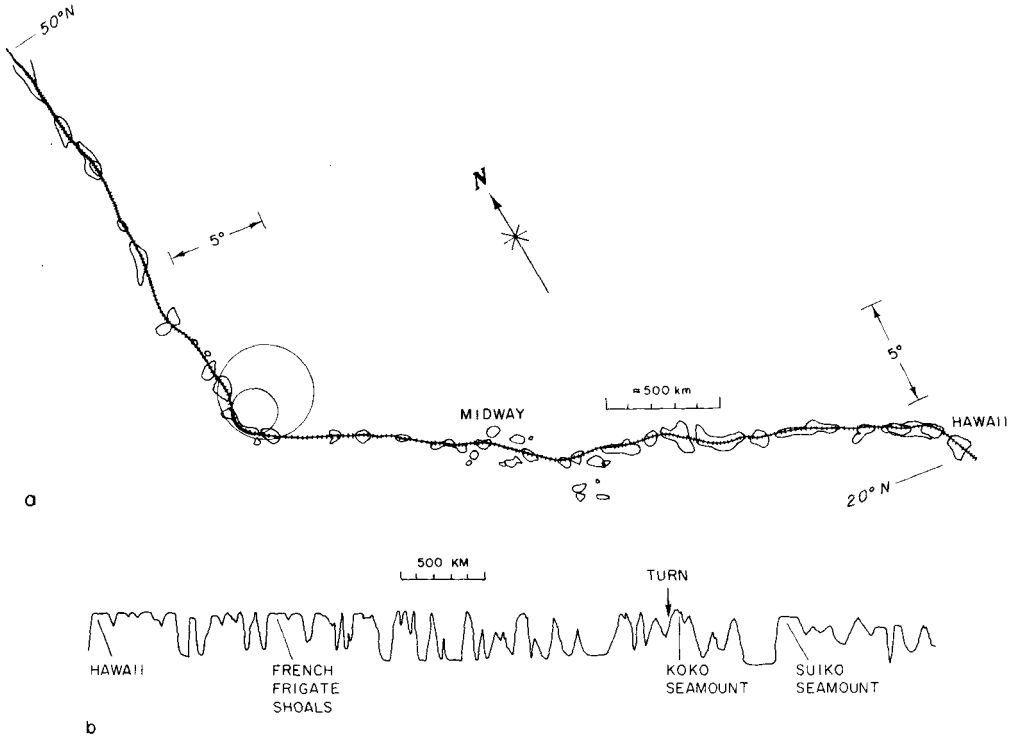

Figure 8. (a) The shallowest track along the Hawaiian Emperor seamount chain. The 1000 m contours are shown. (b) Bathymetry along the shallowest track.

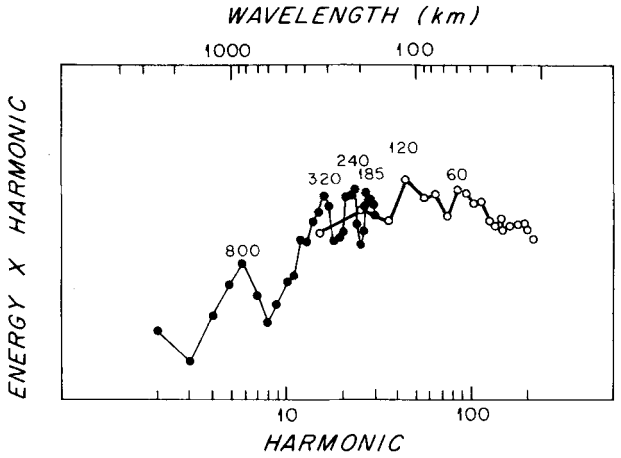

Figure 9. Spectrum of the bathymetry along the shallowest track of the Hawaiian Emperor seamount chain.

shows the spectrum of the bathymetry in Fig. 8(b). It has been smoothed by a ten-point mean for harmonics 10–200 and by a three-point running mean for harmonics 2–30. There is a broad bulge over a k^{-1} slope between wavelengths 45–200 km above which the spectrum begins to level off although there are local peaks at 60, 120, 185, 240, 320 and 800 km wavelengths, respectively. Resolution of the individual volcanoes is beyond the power of this method, but at approximately 30 km a peak would be expected.

We note that if the low viscosity lavas form above the shear zone due to fractionation processes a mechanism of Rayleigh–Taylor instability, as discussed by Marsh (1979), for island arcs may be more relevant to the lavas themselves. In that mechanism the spacing of the magma source is related to the viscosity ratios of the two fluids and the volume of the original magma chamber. Nonetheless the fluid at the shear maximum below the chamber will still be tilted and probably undergo some process like the one described here. Possibly the Marsh mechanism generates the close spacing between individual volcanoes (30 km on average), i.e. there is a Rayleigh–Taylor instability on the tops of 'plume' chambers. Meanwhile, the spacing between islands, which are aggregates of volcanoes, is determined by the processes described here. In such a case the length of the shear zone under plates is still likely to be 100 km or less to be compatible with spacings.

As Skilbeck & Whitehead mentioned, the notion of a shallow slip zone under the plates is not new. A variety of considerations dealing with force balances have recently reinforced this notion (Richter & McKenzie 1978). This is also reinforced by the sharpness of the bend in the Pacific hot spots. For instance, the radius of curvature of the bend in the Hawaiian Emperor seamount chain is somewhere between 100 and 200 km. Unless the hot spot fluid can melt its way directly through the shear zone, it is difficult to reconcile this sharp curvature (see Fig. 8a) with a shear zone over 200 km deep.

Acknowledgments

Support was given to this project from the Geophysics Division, National Science Foundation under grant EAR78-12927. Sincere thanks are extended to Robert Frazel for his valuable work on the experiment. This manuscript is Woods Hole Oceanographic Institution Contribution No. 4882.

References

Anderson, D. L., 1977. Composition of the mantle and core, *Ann. Rev. Earth planet. Sci.*, **5**, 179–202.
Cathles, L. M., III, 1975. *The Viscosity of the Earth's Mantle*, Princeton University Press, 386 pp.
Crough, S. T., 1978. Thermal origin of mid-plate hot-spots wells, *Geophys. J. R. astr. Soc.*, **55**, 451–469.
Dalrymple, G. Brent, Silver, Eli A. & Jackson, Everett D., 1973. Origin of the Hawaiian Islands, *Am. Sci.*, **61**, 294–308.
Marsh, Bruce D., 1979. Island arc development: some observations, experiments and speculations, *J. Geol.*, **87**, 687–713.
McKenzie, D. & Weiss, N., 1975. Speculation on the thermal and tectonic history of the Earth, *Geophys. J. R. astr. Soc.*, **42**, 131–174.
Molner, Peter & Atwater, Tanya, 1973. Relative motion of hot spots in the mantle, *Nature*, **246**, 288–291.
Morgan, W. J., 1971. Convection plumes in the lower mantle, *Nature*, **230**, 42–43.
Morgan, W. Jason, 1972. Deep mantle convection plumes and plate motions, *Bull. Am. Ass. Petrol. Geol.*, **56**, 203.
Murase, T. & McBirney, A. R., 1973. Properties of some common igneous rocks and their melts at high temperature, *Bull. geol. Soc. Am.*, **84**, 3563–3592.
O'Nions, R. K., Hamilton, P. J. & Evensen, Norman M., 1980. The chemical evolution of the Earth's mantle, *Sci. Am.*, **242**, 120–133.
Peltier, W. R., 1976. Glacial-isostatic adjustment – II. The inverse problem, *Geophys. J. R. astr. Soc.*, **46**, 669–705.
Richter, F. M. & Parsons, B., 1975. On the interaction of two scales of convection in the mantle, *J. geophys. Res.*, **80**, 2229–2241.
Richter, F. M. & McKenzie, D., 1978. Simple plate models of mantle convection, *J. geophys. Res.*, **44**, 441–471.
Schubert, G. & Young, R. E., 1976. Cooling the Earth by whole mantle subsolidus convection: a constraint on the viscosity of the lower mantle, *Tectonophys.*, **35**, 201–214.
Schubert, G., 1979. Subsolidus convection in the mantle of terrestrial planets, *Ann. Rev. Earth planet. Sci.*, **7**, 289–342.
Skilbeck, John N. & Whitehead Jr, John A., 1978. Formation of discrete islands in linear island chains, *Nature*, **272**, 499–501.
Stacey, F. D., 1975. Thermal regime of the earth's interior, *Nature*, **255**, 44–45.
Whitehead, Jr, John A. & Luther, Douglas S., 1975. Dynamics of laboratory diapir and plume models, *J. Geophys.*, **80**, 705–717.
Whitehead, Jr, John A. & Parsons, Barry, 1976. Observations of convection at Rayleigh numbers up to 760,000 in a fluid with large Prandtl number. *Geophys. Astrophys. Fluid Dyn.*, **9**, 201–217.
Wilson, J. Tuzo, 1963. A possible origin of the Hawaiian islands, *Can. J. Phys.*, **41**, 863–870.

Appendix: the pressure field outside the conduit due to change in radius

We wish to calculate the pressure field due to a sinusoidal perturbation on a plane interface. The perturbation has velocity W_0 in direction ζ (normal to the interface) and wavenumber k in direction γ. The disturbance on the plane is meant to model an axisymmetrical swelling perturbation on the conduit. The plane geometry affords a simpler solution than the cylindrical geometry and is strictly only valid when ($k \gg r_0^{-1}$). The equations are

$$0 = \frac{-1}{\rho_0}\frac{\partial p}{\partial \gamma} + \nu \nabla^2 u \tag{A1}$$

$$0 = \frac{-1}{\rho_0}\frac{\partial p}{\partial \zeta} + \nu \nabla^2 w \tag{A2}$$

with

$$w = w_0 \sin k\gamma \qquad \text{at} \qquad \zeta = 0$$

$$u = w = 0 \qquad \text{at} \qquad \zeta = \infty$$

$$\frac{\partial u}{\partial \zeta} = \frac{\partial^2 w}{\partial \zeta^2} = 0 \qquad \text{at} \qquad \zeta = 0\,. \tag{A3}$$

A solution for $\nabla^4 w = 0$ with the above boundary conditions is

$$w = W_0 [\sin k\gamma] [1 - k\zeta/2), \exp(-k\zeta). \tag{A4}$$

Thus

$$\frac{\partial p}{\partial \zeta} = W_0 k^2 \mu \exp(-k\zeta \sin k\gamma). \tag{A5}$$

Integrating from infinity to zero

$$p = W_0 k\mu \sin k\gamma$$

and pressure gradient along the conduit is

$$\frac{\partial p}{\partial \gamma} = W_0 k^2 \mu \cos k\gamma\,.$$

The velocity W_0 is the quantity $\partial r/\partial t$ in (3.4).

For a conduit at angle θ, k in this Appendix is equal to the k in the text (in the x-direction) times $\cos\theta$, thus $E = k^2 \cos^2 \theta_0 \mu$.